Sorption and desorption of radioactive organic iodine by silver doped zeolite and zeolite X

Daisuke Akiyama[a,*], Tasuku Ishii[a], Yutaka Masaki[a], Tadashi Narabayashi[b,c], Akira Kirishima[a] and Nobuaki Sato[a]

[a]*Institute of Multidisciplinary Research for Advanced Materials, Tohoku University, 1-1 Katahira, 2, Aoba, Sendai, 980-8577, Japan*
[b]*Graduate School of Engineering, Hokkaido University, Kita-ku, Sapporo, Hokkaido 060-8628, Japan*
[c]*Laboratory for Advanced Nuclear Energy, Institute of Innovative Research, Tokyo Institute of Technology, 2-12-1-N1-16 Ookayama, Meguro-ku, Tokyo, 152-8550, Japan*

Silver doped zeolite (AgX) has attracted significant attention as a good adsorbent of organic iodine (CH_3I) in the gas phase. Heat treatment of the adsorbent waste, which is composed of iodine-sorbed AgX, may be necessary for disposal, as iodine would be removed from AgX at high temperature. Therefore, the sorption and desorption behaviors of CH_3I on AgX and zeolite X (13X) were investigated. Herein, CH_3I labeled by a ^{125}I tracer was synthesized via isotope exchange and used for sorption experiments on AgX. From the sorption experiment results, both labeled $CH_3^{125}I$ and stable CH_3I showed similar sorption behavior and nearly 100% of the CH_3I was sorbed by 5 g of AgX at a flow rate lower than 0.08 m/s. Under high humidity conditions, AgX was soaked and decreased sorption performance was observed. However, after drying the soaked AgX, sorption performance recovered to the initial state. AgX exhibited higher holding performance for iodine than 13X, as almost all of the sorbed iodine was removed from 13X up to 500 °C. In contrast, it was confirmed that removal of the sorbed iodine from AgX was not observed until 830 °C.

1. Introduction

Severe accidents in nuclear power plants have occurred at Chernobyl in 1986, the Three Mile Island nuclear generating station in 1979, and the Fukushima Daiichi nuclear power plant in 2011. A large amount of radioactive materials, including ^{137}Cs and ^{131}I, were released from the reactors to the environment at Chernobyl and Fukushima. Many children and adolescents in the surrounding area in 1986 drank milk contaminated with radioactive iodine, which caused a significant increase in the incidence of thyroid cancer. In contrast, IAEA reported that increased incidence of thyroid cancer has been indiscernible around Fukushima, because it is difficult to assess such a small incidence against the normal statistical fluctuations in cancer incidence [1]. Filtered containment venting systems (FCVSs) is an example of an emergency response system for severe nuclear accidents [2, 3].

On the other hand, a mock-up of high efficiency multi-nuclide aerosol filtration system has been developed for reducing the radiation dose of internal exposure for workers in the decommissioning activity of Fukushima Daiichi nuclear power plant [4]. This system consists of a dry or wet filter for collecting radioactive dust and fumes, in addition to a silver doped zeolite filter for capturing radioactive gas including ^{129}I. Both systems are designed to remove radioactive nuclides released from the reactor and containment vessels [2-4]. Iodine exists in a variety of chemical forms including I_2 and CH_3I in the gas phase and I^- and IO_3^- in the liquid phase [5-12]. I_2 in ventilation gas easily dissolves in water along with other water-soluble ions by wet filtration. However, water insoluble species, such as CH_3I, are also contained in ventilation gas [13]. Then some sorbents for organic iodine such as TEDA doped activated charcoal and silver doped zeolite have been

studied. The TEDA doped activated charcoal is one of the promising sorbent for organic iodine, however, it couldn't be used at high temperature due to its flammability, while silver doped zeolite (AgX) is a very promising sorbent for CH_3I since it can remove >99.99% of CH_3I in vent gas and can be used at high temperature [14-17]. Studies regarding the sorption of iodine from reprocessing plant off-gas streams including dissolution, vessel, melter, and cell off-gases by silver-doped zeolite have been extensively reported [18-26]. The mechanism of silver-loaded adsorbents trapping iodine has been known for a long time [27-30]. Furthermore, high efficiency multi-nuclide aerosol filters for radiation protection systems are used during core cutting under high humidity conditions due to the high humidity in the containment vessels of the Fukushima Daiichi nuclear power plant. The performance of silver zeolite sorbents for CH_3I has been investigated under high humidity conditions [31]. Herein, the sorption of CH_3I by AgX under high humidity conditions and that of dried AgX were performed. Ag-based sorbents are known to capture $I_2(g)$ or $CH_3I(g)$ to form solid AgI immobilized in AgX [32-34]. The adsorbent waste (iodine-sorbed AgX) must be treated prior to disposal. The suitable waste forms include crystal matrix, glass, aerogels, and cement [35]. It is also necessary to heat the adsorbent waste of the crystal matrix by Hot Isostatic Pressing (HIP) solidification [36, 37] and glass processes [38, 39]. Thus, it is necessary to assess the desorption behavior of iodine from AgX at high temperatures. The desorption test for iodine from silver-mordenite has been previously reported but was performed up to 600 °C [40, 41]. Choi et al. also reported that iodine from 13X after the sorption test could be removed, while iodine from AgX was not removed at 650 °C [5]. However, these temperatures are insufficient to assess the desorption behavior of iodine from AgX. The AgX was synthesized by doping silver to 13X zeolite which is a type of zeolite X. In this study, therefore, 13X was also used for

*Corresponding author. d.akiyam@tohoku.ac.jp

comparing the iodine desorption behavior with AgX. Thus, desorption tests using the iodine-sorbed AgX and 13X were performed at a higher temperature, 950 °C. In addition, degassing from the iodine-sorbed AgX at high temperature was analyzed by Mass spectrometry (MS).

2. Experimental

2.1. Materials

2.1.1 Preparation of 13X zeolite and AgX. The 13X zeolite (Union Showa K.K.) is a type of zeolite X and its composition is $Na_{86}[(AlO_2)_{86}(SiO_2)_{106}] \cdot 276H_2O$. The AgX was manufactured by Rasa Industries using the 13X zeolite wherein sodium was substituted with silver. The silver ion exchange ratio was ≥97%, the silver content when dried was ≥36 wt%, particle size of 10 × 20 mesh, and the water content was ≤12 wt% as estimated by the weight reduction when the AgX was dried at 150 °C for 3 h [14].

2.1.2 Radioactive $CH_3{}^{125}I$. The ^{125}I in 0.1 M NaOH was obtained from PerkinElmer. The CH_3I labeled with ^{125}I was synthesized via isotope exchange reaction between ^{125}I in 0.1 M NaOH solution and water insoluble CH_3I [32, 42];

$$Na^{125}I + CH_3I \rightleftharpoons CH_3{}^{125}I + NaI \qquad (1)$$

The two phases were contacted for 20 h and the γ-ray released from ^{125m}Te that is the decay product of ^{125}I was measured by NaI(Tl) scintillation detector. The exchange ratio (R) was obtained by the following equation;

$$R = W_2 / W_1 \times V_1 / V_2 \times 100 \qquad (2)$$

where R is the exchange ratio (%), W_1 is the count of ^{125}I injected (cps/mL), W_2 is the counts of ^{125}I exchanged to CH_3I (cps/mL), V_1 is the volume of $Na^{125}I$ (mL), and V_2 is the volume of CH_3I (mL).
The detailed procedure and time dependence of the exchange ratio were reported previously [32]. The CH_3I labeled by ^{125}I with an exchange ratio of 10% was used in this study.

2.2. Sorption experiment. The sorption experiment was performed using radioactive methyl iodide ($CH_3{}^{125}I$) and the stable form in the two types of experimental systems, as shown in Figure 1. A PYREX glass apparatus was used at gas flow rates of lower than 500 mL/min, whereas a stainless-steel apparatus was used at rates of higher than 500 ml/min with steam condition. The experimental conditions of using glass apparatus and stainless-steel apparatus are shown in Tables 1 and 2, respectively. The glass apparatus system was composed of three parts, i.e. 1) the $CH_3{}^{125}I$ injection, 2) Tube 1: the sorption tube with AgX or 13X doped zeolite (5 g), Tube 2: the
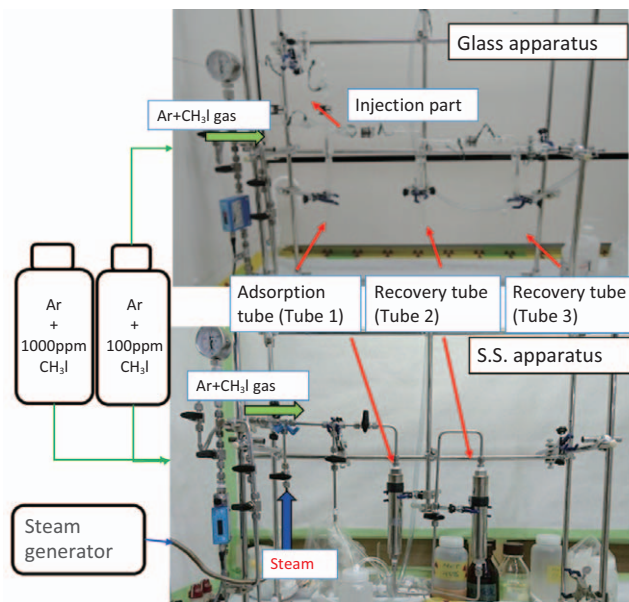

Figure 1. Experimental system using glass and the stainless-steel (S.S.) apparatus.

recovery tube for un-trapped CH_3I, and 3) Tube 3: the additional recovery tube for un-trapped CH_3I. First, 15 mL of 99 wt% ethanol and 15 mL of 50 wt% ethanol were filled in Tubes 2 and 3, respectively, to trap CH_3I that passed through Tube 1. Ar + 100 ppm CH_3I gas flowed at 20 to 500 mL/min for 1 h during the sorption test. When using radioactive methyl iodide ($CH_3{}^{125}I$), 1.0 mL of $CH_3{}^{125}I$ was injected and flowed to Tube 1 for 1 h via a carrier gas (Ar) at a flow rate of 500 mL/min. After the sorption test, the stable iodine concentrations in the solutions in Tubes 2 and 3 were measured by ICP-AES, whereas the radioactive iodine concentration was measured using a NaI scintillation counter. The stainless-steel apparatus system was composed of three parts, i.e. 1) Tube 1: the sorption tube with AgX doped zeolite, 2) Tube 2: the recovery tube for un-trapped CH_3I, and 3) AgX was filled in Tube 2 to trap CH_3I that passed through Tube 1. Ar + 100 ppm CH_3I and Ar + 1000 ppm gases flowed at 500 to 1000 mL/min for 1 h for the sorption test. To evaluate the effects of steam on the sorption, a steam generator (Nihon dennetsu, K007) was used and steam was introduced at an oversaturated vapor partial pressure. After the sorption test, the sorption amount of stable iodine in the AgX in Tube 1 was measured by X-ray Fluorescence (XRF, Rigaku, Supermini 200). In addition, the iodine-sorbed AgX after the sorption test with steam was removed from Tube1 and dried using vacuum drying system for 1 day. The dried AgX was used for the second sorption test without steam. To compare sorption ratios using the

TABLE 1: Sorption experimental conditions at flow rates of lower than 500 mL/min using a PYREX glass apparatus.

AgX in tube1 (g)	Tube 1 temperature (°C)	Concentration of CH_3I	Ar+100 ppm CH_3I gas flow rate	
			(mL/min)	(m/s)
5	25 (Room temperature)	Ar+100 ppm CH_3I	50	0.014
			100	0.027
			200	0.055
			300	0.082
			400	0.109
			500	0.137
		5.2×10^5 ppm in Ar (saturated CH_3I) Incl. 60 Bq ^{125}I	500 (Ar gas flow rate)	0.137 (Ar gas flow rate)

TABLE 2: Sorption experimental conditions at flow rates of higher than 500 mL/min using a stainless steel apparatus.

AgX in tube 1 (g)	Tube 1 temperature (°C)	Ar+100 ppm CH$_3$I		Ar+1000 ppm CH$_3$I		Saturated water condition
		Gas flow rate		Gas flow rate		
		mL/min	m/s	mL/min	m/s	
		500	0.016	-	-	-
		-	-	500	0.016	
		500	0.016	-	-	With steam
		-	-	500	0.016	
5	25 (Room temperature)	-	-	750	0.024	-
						With steam
		1000	0.031	-	-	-
		-	-	1000	0.031	
		1000	0.031	-	-	With steam
		-	-	1000	0.031	

PYREX glass and stainless-steel equipment, the flow rate unit, mL/min, was converted to m/s using Eq. (3);

$$\text{Flow rate (m/s)} = \text{Flow rate (m}^3\text{/s)} / \text{Cross-sectional area in Tube 1 (m}^2) \quad (3)$$

The cross-sectional area in PYREX glass Tube 1 was 6.1×10^{-5} m^2 and that of the stainless-steel was 5.3×10^{-4} m^2.

2.3 Desorption experiment. To evaluate the desorption of iodine sorbed onto AgX and 13X, saturated iodine-sorbed AgX and 13X were prepared by supplying CH$_3$I to AgX and 13X until reaching the sorption saturation state. To evaluate the apparent sorption capacity of AgX and 13X, breaking through experiment was carried out in our former study [32]. The apparent sorption capacity of CH$_3$I on AgX and 13X at 24 °C were evaluated to be 0.21 g/g and 0.56 g/g, respectively. Then, the saturated iodine-sorbed AgX and 13X were evaluated by thermogravimetric and differential thermal analyses (TG-DTA, Thermo plus 2, Rigaku) measurements, where the composition of the degas from the furnace of TG-DTA was analyzed by quadrupole mass spectrometer (M-201GA-CRMY, Rigaku). First, the saturated iodine-sorbed AgX and 13X were heated to 500 °C, which is under melting point of AgI (552 °C), by a heating rate of 10 °C/min to remove water adsorbed to the AgX and 13X from the atmosphere. After cooling, the samples were heated again to 950 °C by a heating rate of 10 °C/min in Ar. For comparison, reagent grade AgI was measured under the same conditions. For the quadrupole MS, He gas was flowed at 500 mL/min before heating until the intensities of the elemental mass-to-charge ratio (*m/z*) derived from air, i.e. *m/z*= 18 (H$_2$O), 28 (N$_2$) and 32 (O$_2$) decreased sufficiently. After the background ions decreased to constant low intensities, saturated iodine-sorbed AgX and AgI regent (Sigma-Aldrich, 99.999%) were heated to 1400 °C and 950 °C, respectively, by a heating rate of 20 °C/min. The intensities of the elemental *m/z* of 18 (H$_2$O), 63 (I), and 127 (I$_2$) were measured during the heating.

3. Results and discussion

3.1. Sorption of CH$_3$I on AgX. Figure 2 shows the relation between the sorption ratio and gas flow rate. When the gas flow rate was lower than 0.08 m/s, almost 100% of the CH$_3$I was sorbed and at flow rates of higher than 0.08 m/s, the sorption ratio of CH$_3$I decreased to lower than 50% at 0.14 m/s. Using radioactive methyl iodide (CH$_3$^{125}I), the sorption ratio at a 0.14 m/s flow rate was similar. Under steam conditions, the
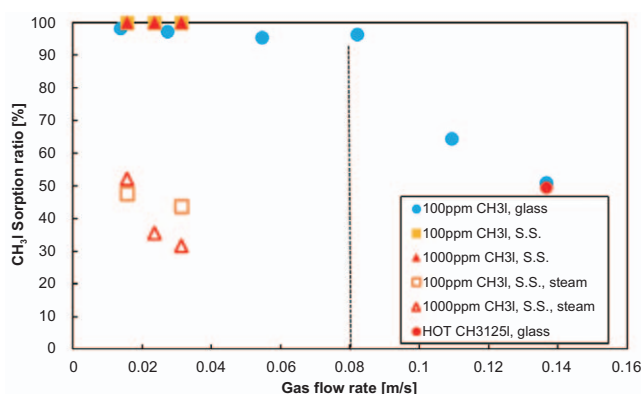

Figure 2. Relation of the sorption ratio and gas flow rate [m/s] under various conditions.

CH$_3$I sorption ratio decreased to the range of 30% to 50%. At faster flow rates, the sorption ratio decreased with the oversaturated vapor partial pressure. Because some steam became water and soaked into AgX in Tube 1, CH$_3$I was prevented from sorbing on AgX. From a previous study, it is recognized that the apparent sorption capacity of AgX decreased with 3% H$_2$O in Ar [24]. When water was contained in the flowed gas, the sorption ratio and sorption capacity decreased. In addition, the soaked AgX was dried and recycled for another sorption test, confirming that the sorption performance was restored to that of the initial state.

3.2. Thermal stability of iodine-sorbed AgX or 13X. The saturated iodine-sorbed AgX and 13X were analyzed by TG-DTA. The obtained TG-DTA curves of the AgX sample heated from room temperature to 500 °C is shown in Figure 3(a). After the above mentioned procedure, this sample was cooled down to room temperature and again heated to 950 °C by 10 °C/min. The TG-DTA curves of this heat treatment are shown in Figure 3(b). Figure 3(a) shows the gradual endo-thermic reaction from room temperature to 100 °C and the decreasing weight due to volatilizing adsorbed water. The adsorbed water in AgX is known to volatilize up to 500 °C [6]. Figure 3(b) shows a slight decreasing TG curve. The limited amount of iodine volatilized from the AgX up to 800 °C. But over 830 °C, a remarkable weight decrease was observed due to the decomposition of AgI and volatilization of I$_2$ as following Eq. (4).

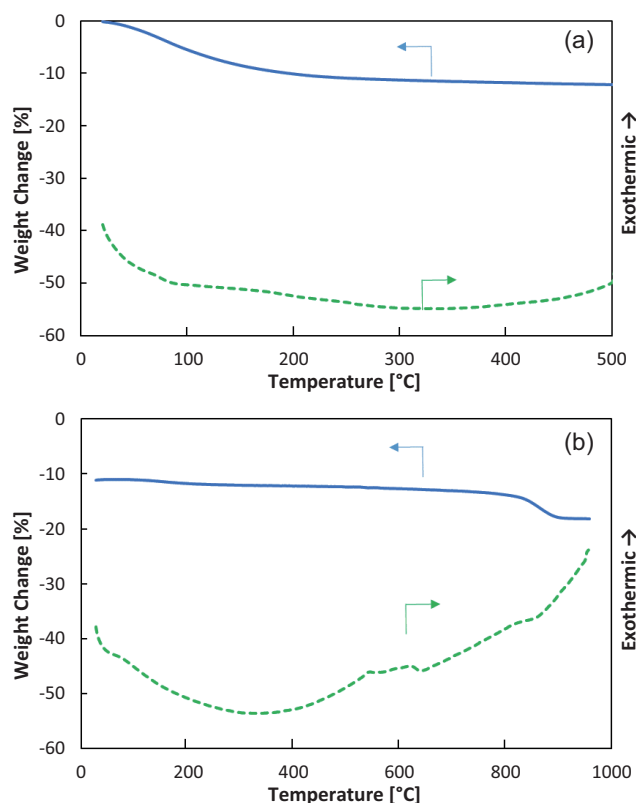$$2AgI \rightarrow 2Ag + I_2 \quad (4)$$

Figure 3. (a) TG-DTA curves of the saturated iodine-sorbed AgX at a 10 °C /min heating rate to 500 °C under flowing Ar gas. (b) TG-DTA curves of the dried saturated iodine-sorbed AgX at a 10 °C /min heating rate to 950 °C under flowing Ar gas.
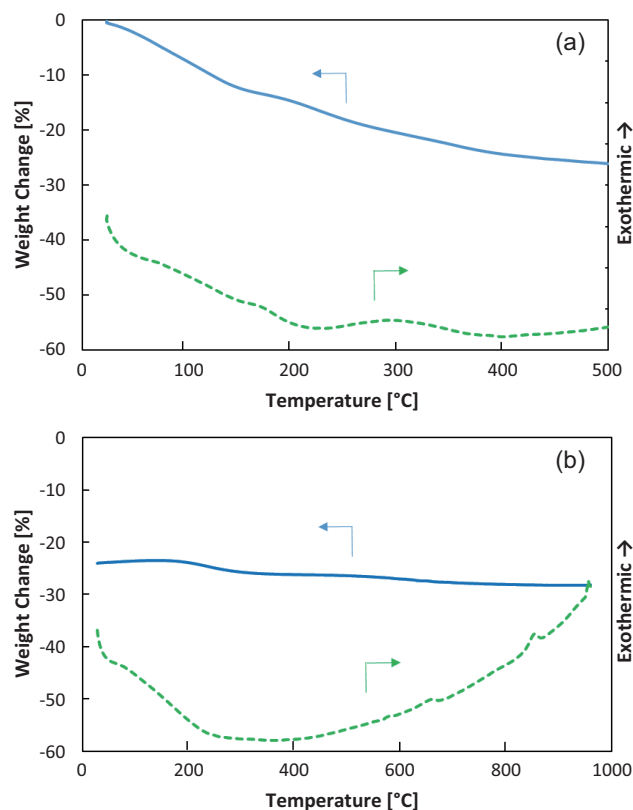

Figure 4. (a) TG-DTA curves of saturated iodine-sorbed 13X at a 10 °C /min heating rate to 500 °C under flowing Ar gas. (b) TG-DTA curves of dried saturated iodine-sorbed 13X at a 10 °C /min heating rate to 950 °C under flowing Ar gas.

The TG-DTA curve to 500 °C of the saturated iodine-sorbed 13X is shown in Figure 4(a). After the 1st TG-DTA measurement, the 13X sample was cooled down to room temperature. Then, the sample was again heated to 950 °C to obtain 2nd TG-DTA curve shown in Figure 4(b). Figure 4(a) shows continuous weight decrease, which was supposed to attribute to the volatilization of sorbed water and iodine in the 13X sample. The weight change caused by the desorption of water in 13X was evaluated by additional experiment, that is, the TG-DTA measurement for initial 13X sample which was not contacted with CH_3I. The TG curve of this additional experiment indicated that approximately -5% of weight change was caused by the desorption of water in 13X (Figure S1). Hence, we concluded that the weight decreases in Figure 4(a) caused by the iodine volatilization from the 13X sample was much larger than that caused by the water volatilization. Figure 4(b) shows the slight weight decrease in comparison with that shown in Figure 4(a) because almost all of the iodine had already volatilized in the 1st TG-DTA measurement up to 500 °C. These results indicate that AgX fixed iodine up to 830 °C, while the 13X released whole sorbed iodine up to 500 °C. This result evidentially indicates that AgX has higher iodine fixation ability than that of 13X.

The TG curve and MS signals (H_2O, I, and I_2) of AgI by 20 °C/min heating to 950 °C in He atmosphere are shown in Figure 5. The weight was almost constant up to 750 °C, and at the higher temperature, the weight decreased sharply up to 930 °C. Peaks of MS signals corresponding to I and I_2 were observed at 890 °C, while the other MS signals, such as H_2O, were temporally disturbed for large amount of I and I_2 being released from the sample AgI due to saturation of the MS spectrometer. This indicates that AgI was stable up to 750 °C, but at higher temperature AgI was decomposed to Ag and I_2. The TG curve and MS signals (H_2O, I, and I_2) of the saturated iodine-sorbed AgX by 20 °C/min heating to 1400 °C in He is
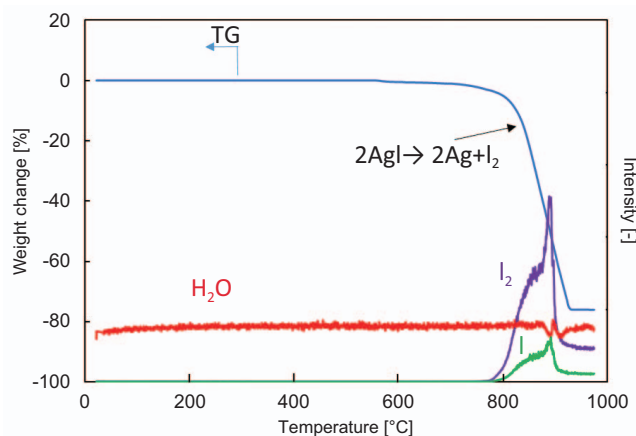

Figure 5. TG curve and MS intensity (H_2O, I, and I_2) of the AgI reagent at a 20 °C /min heating rate to 950 °C under flowing He gas.

shown in Figure 6. The weight decrease was observed from 30 °C to 250 °C in the TG curve while two peaks were found in MS signals of H_2O at 100 °C and 200 °C. This result is interpreted as two types of sorbed water existed in the AgX, that is, water molecules in surface and those in channels of the AgX. At 830 °C, the weight decreased sharply and MS signals corresponding to I_2 were observed, which seems to be caused by AgI decomposition and iodine volatilization. This decomposition temperature was slightly higher than that observed in the pure AgI experiment. Thus, AgI in AgX matrix was thermally stabilized in comparison with pure AgI., However, this stabilization effect is minor since the framework of zeolite X collapses at 843 °C [43]. At temperatures higher than 1200 °C, the weight decreased gradually without MS signals of H_2O, I, and I_2, which indicated that this weight change was caused by the decomposition of the AgX matrix.
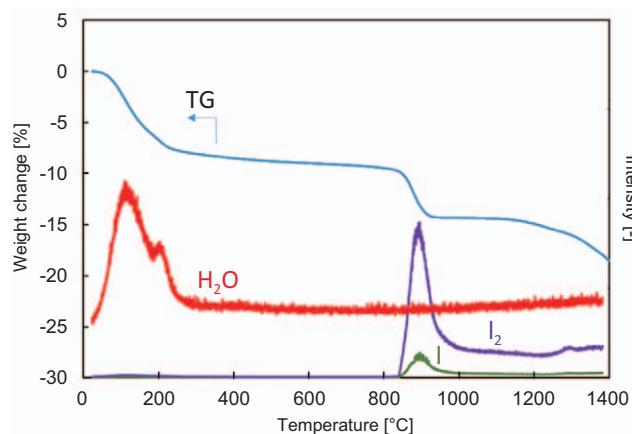
Figure 6. TG curve and MS intensity (H_2O, I, and I_2) of saturated iodine-sorbed AgX at a 20 °C/min heating rate to 1400 °C under flowing He gas.

4. Conclusion

Herein, radioactive $CH_3{}^{125}I$ was synthesized and its sorption on AgX was examined. Both labeled $CH_3{}^{125}I$ and stable CH_3I showed similar sorption behaviors. When the flow rate of Ar + CH_3I gas was lower than 0.08 m/s, almost all of the CH_3I (>99.9%) was adsorbed by 5 g AgX. Upon introduction of steam and soaking AgX, the sorption ratio decreased, but drying the soaked AgX restored the sorption performance to the initial state. Using saturated iodine-sorbed AgX and 13X, both sorbents could adsorb iodine. However, almost all of the sorbed iodine was removed from 13X up to 500 °C, whereas AgX retained the iodine up to 830 °C. This temperature is similar to the decomposition temperature of AgI. Thus, the thermal stability of iodine captured by AgX was determined to be similar to that of AgI powder.

Acknowledgments

References

[1] International Atomic Energy Agency, *The Fukushima Daiichi Accident*. (IAEA, Vienna, 2015).

[2] G. Verreck, C. Schweinheim, P. Hunten, H. Martinsteg, P. Hausch, H. Likar, *Filtered Venting of the Containment of Nuclear Power Plants (The Dry Filter Method)*, (YIT Germany GmbH, 2011).

[3] Working group of Filtered Containment Venting System, *Filtered Containment Venting System*. (ERC publishing company, 239, ISBN 4900622613, 2018) (in Japanese).

[4] T. Narabayashi, *Development of a High Efficiency Multi–nuclide Aerosol Filters for Radiation Protection during a Process of Cutting Core, the Nuclear Energy Science & Technology and Human Resource Development Project (through concentrating wisdom) (2017)*. https://iss.ndl.go.jp/books/R100000002-I029092186-00 (accessed on 27 Jan. 2021) (in Japanese).

[5] B.S., Choi, G. I. Park, J. H. Kim, J. W. Lee, and S. K. Ryu, Adsorption **7**(2), 91 (2001).

[6] B. Clément, L. Cantrel, G. Ducros, F. Funke, L. Herranz, A. Rydl, G. Weber, and C. Wren, *State of the Art Report on Iodine Chemistry.* (OECD Nuclear Energy Agency Report NEA/CSNI/R, 2007).

[7] B. Simondi-Teisseire, N. Girault, F. Payot, and B. Clément, Ann. Nucl. Energy **61**, 157 (2013).

[8] L.E. Herranz and B. Clément, Prog. Nucl. Energy **52**, 481 (2010).

[9] L. S. Level, R. S. Dickson, and G. A. Glowa, J. Environ. Radioactiv. **151**, 82 (2016).

[10] N. Momoshima, S. Sugihara, R. Ichikawa, and H. Yokoyama, J. Environ. Radioactiv. **111**, 2 (2012).

[11] G. Katata, M. Chino, T. Kobayashi, H. Terada, M. Ota, H. Nagai, M. Kajino, R. Draxler, M. C. Hort, A. Malo, T. Toriim and Y. Sanada, Atmos. Chem. Phys. **15**, 1029 (2015).

[12] A. Mathieu, M. Kajino, I. Korsakissok, R. Périllat, D. Quélo, A. Quérel, O. Saunier, T. T. Sekiyama, Y. Igarashi, D. Didier, Appl. Geochem. **91**, 122 (2018).

[13] U.S. Nuclear Regulatory Commission., Regulatory Guide 1.195 (2003).

[14] T. Kobayashi, K. Endo, U. S. Patent 2018/0029007 A1.

[15] H. Xiao, J. Liu, Nucl. Power Eng., **21**(4), 357 (2000).

[16] A. Sultana, M. Sasaki, K. Suzuki, H. Hamada, Appl. Catal., A., **466**, 179 (2013).

[17] M. K. Kim, P. S. Kim, J. H. Baik, I. S. Nam, B. K. Cho, S. H. Oh, Appl. Catal., B., **105** (1-2), 1 (2011).

[18] T. Sakurai, M. Izumo, A. Takahashi, Y. Komaki, J. Nucl. Sci. Technol., **20**(3), 264 (1983).

[19] T. Sakurai, M. Izumo, A. Takahashi, Y. Komaki, J. Nucl. Sci. Technol., **20**(9), 784 (1983).

[20] T. Sakurai, M. Izumo, A. Takahashi, Y. Komaki, J. Nucl. Sci. Technol., **20**(12), 1046 (1983).

[21] R.T. Jubin, S.H. Bruffey, B.B. Spencer, Proceedings of Global 2015, (France, 2015), Paper 5223.

[22] R.T. Jubin, ORNL/TM-6607, Oak Ridge National Laboratory, Oak Ridge, TN. (1979).

[23] W. Hebel, G. Cottone (Eds.), Radioactive Waste Management, Vol. 7: Management Modes for Iodine-129, Harwood Academic Publishers, Brussels, Belgium (1982).

[24] IAEA, TRS-276, International Atomic Energy Agency, Vienna, Austria (1987).

[25] IAEA, IAEA-TECDOC-1744, International Atomic Energy Agency, Vienna, Austria (2014).

[26] L. L. Burger, R.D. Scheele, PNNL-14860, Pacific Northwest National Laboratory, Richland, WA (2004).

[27] C. J. Li, YJ Li, J.N. Wang, L. Zhao, J. Cheng, Chem. Eng. J., **222**, 419 (2013).

[28] C. Liu, R. Mallinson, L. Lobban, Appl. Catal., A., **178**(1), 17 (1999).

[29] J. W. Lacksonen, W. H. Kirby, C. E. Dryden, J. Chem. Eng. Data, **8**(4), 524 (1963).

[30] K. C. Patil, C. N. R. Rao, J. W. Lacksonen, C. E. Dryden, J. Inorg. Nucl. Chem., **29**(2), 407 (1967).

[31] G. Y. SooHoo; Chien-chang Lin; R. M. Norris; C. D. Wilkinson, IEEE Trans. Nuclear Sci. **22**(1), 657 (1975).

[32] T. Ishii, D. Akiyama, A. Kirishima, N. Sato, T. Narabayashi, proceedings of 24th International Conference on Nuclear Engineering (ICONE 24, 2016).

[33] S. Matsuoka, H. Nakamura, T. Tamura, T. Takano, Y. Ito, J. Nucl. Sci. Technol. **21**(11), 862 (1984).

[34] K. W. Chapman, P. J. Chupas, T. M. Nenoff, J. Am. Chem. Soc., **132**(26), 8897–8899 (2010).

[35] Riley, B. J., et al., Materials and processes for the effective capture and immobilization of radioiodine: A review. J. Nuclear Mater. 470, 307–326 (2016).

[36] R.T. Jubin, CONF-811108-14, Oak Ridge National Laboratory, Oak Ridge, TN (1981).

[37] R.T. Jubin, S. H. Bruffey, K.K. Patton, FCRD-SWF-2014e000278, ORNL/LTR-2014/476, Oak Ridge National Laboratory, Oak Ridge, TN (2014).

[38] P. Wesolowski, W. Jakubowski, J. L. Nowiński, Phys.

Status Solidi A **115**(1), 81 (1989).

[39] T. Minami, Y. Ikeda, M. Tanaka, J. Chem. Soc. Jpn. **10**, 1617 (1981) (in Japanese).

[40] T. M. Nenoff, M. Rodriguez, N. Soelberg, K. Chapman, Proceedings of Global 2015, (France, 2015), Paper, 5055.

[41] T. M. Nenoff, M. A. Rodriguez, N. R. Soelberg, K. W.

Chapman, Microporous Mesoporous Mater. **200**, 297 (2014).

[42] K.B. Sung, H. Y. Yang, J. H. Lee, J. S. Choi, T. W. Hwang, US Patent 2012/0209035 A1, 201.

[43] D. Chen, X. Hu, L. Shi, Q. Cui, H. Wang, H. Yao, Appl. Clay Sci., **59–60**, 148 (2012).
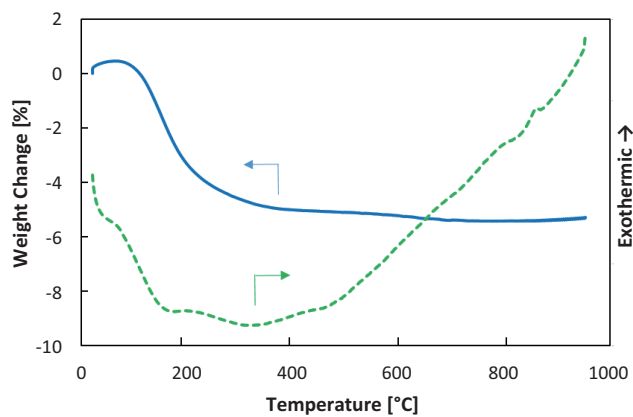
Appendix

Figure S1. TG-DTA curves of 13X at a 10 °C/min heating rate to 950 °C under flowing Ar gas.